13th Int Symp on Applications of Laser Techniques to Fluid Mechanics
Lisbon, Portugal, 26-29 June, 2006
Paper No. #1301

Extension of the compressed interferometric particle sizing technique for three–component velocity measurements

Daisuke Sugimoto[1], Konstantinos Zarogoulidis[2], Tatsuya Kawaguchi[3], Kazuaki Matsuura[4], Yannis Hardalupas[2], Alex M.K.P. Taylor[2], Koichi Hishida[1]

1: Dept. of System Design Engineering , Keio University, Yokohama, Japan, sugimoto@mh.sd.keio.ac.jp
2: Dept. of Mechanical Engineering, Imperial College, London, UK, konstantinos.zarogoulidis@imperial.ac.uk
3: Dept. of Mechanical and Control Engineering, Tokyo Institute of Technology, Tokyo, Japan, kawat@mep.titech.ac.jp
4: Japanese Aerospace Exploration Agency, Tokyo, Japan, matsuura.kazuaki@jaxa.jp

Abstract The present contribution extends the presently planar advanced interferometric laser imaging particle sizing technique with compressed fringe patterns to measuring the third velocity component of particles present in two phase flows. Two different methodologies are investigated to measure the depth velocity; one employing just one camera and the other a two–camera stereoscopic arrangement. Both employ optical compression systems to increase particle number concentration per image. The first method, one-camera arrangement, calculates the particle depth position via its fringe pattern length. The relationship between the depth position and the fringe pattern length is constructed by traversing a monodisperse droplet generator inside the measurement volume. The resolution along the depth–direction was found to be 140μm when a one–pixel change occurs in the fringe pattern length, which is low given the uncertainty of the fringe length estimation. For the stereoscopic arrangement, the 3D position is determined by matching the compressed fringe patterns for each particle on both views and determining their depth position from the calibration mapping information. To verify the accuracy of the three–component velocity, a monodisperse generator was inclined relative to the laser sheet plane. Regarding the size measurement, the mean droplet diameter was estimated with an error of 2.6%. The results from the spray measurement confirmed the applicability of the proposed stereoscopic instrument. As a conclusion, the stereoscopic arrangement proposed is a capable instrument for accurately measuring the sizes and the three–component velocity of particles in two–phase flows.

1. Introduction

Many processes in industrial and every–day life applications involve liquid particles. Examples include — but are not limited to — fuel injection in combustion systems, spray inhalers in medical applications and ink–jet printers. The better understanding and optimization of such processes is very important. A case of special interest is combusting sprays, where engine performance and emissions are directly affected by the quality of the spray injector atomisation. It is therefore clear that the development of capable tools that can help in the design and optimisation of such systems is a necessity.

To investigate liquid particle systems, the size and velocity distributions of the individual particles are required for detailed analysis of the flow structure and characteristics. Many instruments have been proposed for the measurement of these parameters. The most commonly used are point measurement systems with the most representative being the Phase Doppler Anemometer (PDA). The PDA utilises the properties of the light scattered by the particles. The particle size and velocity information is extracted from the scattered light phase as particles traverse the probe volume that two intersecting beams form. The main disadvantage of the PDA is that many measurements are required for analysis of the flow dynamics in a large measurement volume due to its point measurement nature. Due to this, flow visualisation is not as easy as with imaging techniques that are capable to instantly visualise a relatively large area of the flow.

Interferometric laser imaging droplet sizing (ILIDS) is a planar measurement technique that overcomes this difficulty. ILIDS provides the instantaneous spatial, size and planar velocity

distribution of the particles by analysing the interference pattern created by the reflected and refracted rays that originate from the surface of each particle (Glover *et al*. 1995). The size of the particle is given by the angular frequency of its fringe pattern (Hesselbacher *et al.* 1991) or alternatively, the number of fringes in the pattern. In addition, the two–dimensional velocity information is readily available by estimating the individual particle displacement between consequent images using traditional Particle Tracking Velocimetry (PTV) methodology. Traditional ILIDS image processing is hindered by fringe pattern overlapping in dense particle areas, making the particle identification process a difficult task. To cater for the fringe overlapping problem, Maeda *et al*. (2000) introduced an optical compression system that reduces the circular fringe patterns produced by ILIDS to line fringe patterns (**Fig. 1**). Application of this optical compression system increases significantly the droplet number density per image and therefore the instrument applicability in dense particle flows.

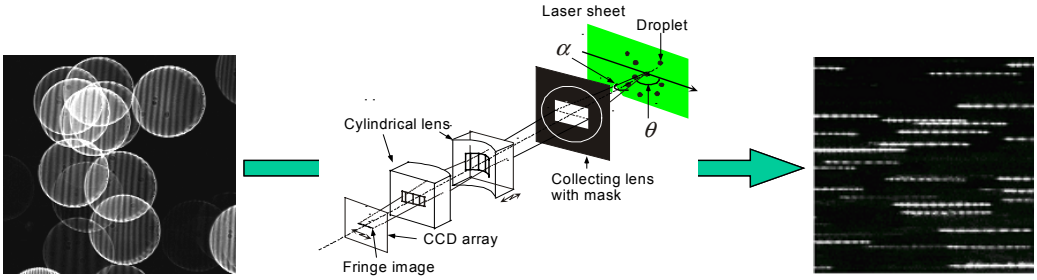

Fig 1. Optical arrangement of the advanced interferometric imaging technique

As mentioned, ILIDS is capable of measuring particle size and two–dimensional velocity information. Even though this capability is a clear advantage over the PDA, there are particle flows where three–dimensional motion is very important, such as strong swirl flows. Recently, instruments based on the same sizing measurement principle to the one ILIDS have been proposed, capable of measuring particle size and three–component velocity simultaneously (Damaschke et al. 2001, Zama *et al*. 2004). These systems employ stereoscopic arrangements of one out–of–focus camera for the sizing processing and a second in–focus camera for particle tracking and verification. This approach has two disadvantages. The first is that the particle validation is achieved by estimating the bright spot distance on the surface of the particles and such an estimation carries an inherited uncertainty due to the lack of sufficient resolution in present typical imaging systems. The second is that both employ the traditional uncompressed fringe patterns, making overlapping a serious issue in dense particle areas. Due to the above, the development of a new measurement instrument for measuring the size and three–component velocity of particles in dense flow is viable.

In the present contribution two different methods to determine the size and three–dimensional location of particles in regions with high number density concentrations are considered. The first method calculates the depth position via the particle fringe pattern length, while the second by locating the particle in two camera views and extracting the depth–velocity from the combined information like stereoscopic PIV. These methods are applied for a piezoelectric mono–disperse generator and the stereoscopic arrangement approach is in addition applied for a typical spray in a swirling flow. The results are discussed and evaluated.

2. Measurement Technique

2.1 Sizing and planar velocity measurement by interferometric laser imaging technique

When light illuminates a spherical droplet, there is an angular region (for water, 20°~80° to the

forwardly–propagating light) in which only reflected and first–order refractive rays are emanated from the droplet surface. Due to these two rays, in the focal image plane two very bright spots (glare points) are observed (Van de Hulst and Wang 1991). Although the distance between the glare points is proportional to the particle size, evaluating the size from this distance is difficult due to the lack of the adequate resolution in conventional imaging equipment. On a non–focal plane, the two rays interfere with each other and an interferogram can be observed. ILIDS measures the diameter of a spherical transparent particle from the fringe undulation frequency or the number of independent of the absolute light intensity (Hesselbacher *et al.* 1991, Roth *et al*. 1991).The relationship between the two is derived by the phase difference between reflection and first–order refraction rays originating from the droplet. The relation between the particle diameter d and the number of fringes N is given by the equation

$$d = \frac{2\lambda N}{\alpha}\left[\cos\frac{\theta}{2} + m\sin\frac{\theta}{2}\cdot\left(m^2+1-2m\cos\frac{\theta}{2}\right)^{-\frac{1}{2}}\right]^{-1}, \qquad (1)$$

where λ is the laser light source wavelength, m is the relative refractive index of the liquid droplet, θ and α are the scattering and the collecting angles respectively (Maeda *et al*., 2000). Due to their circular shape, fringe pattern recognition in the conventional ILIDS technique is difficult or even impossible due to pattern overlapping in high particle concentration regions. Fig. 1 illustrates the optical arrangement of the advanced interferometric laser imaging technique which aims at increasing the particle number density and to simplify the imaging processing procedure. It comprises of a pair of cylindrical lenses placed between the imaging plane and the objective lens in order to project the horizontal out–of–focus images on a vertically focused plane (Maeda *et al.* 2000, 2002, Kawaguchi *et al.* 2002). The cylindrical lens can be moved along the optical axis of the receiving optics enabling adjustment of the horizontal defocusing degree. By using the "squeezing" optical system, the degree of fringe pattern overlapping in the resulting images has been drastically reduced which in turn increases the applicability of the instrument in real–world applications.

In addition to the instrument's sizing capabilities — following common PTV practice — the two–dimensional velocity is measured in consequent frames using cross–correlation. In conjunction to the cross–correlation coefficient, the validity of the planar displacement estimation can be validated by comparing the particle size of the particle in the first frame to the size of the candidate particles inside the predefined interrogation window.

As already mentioned, evaluation of the three–component velocity is of importance. To determine the three–dimensional droplet location and velocity, two methodologies can be applied. The first utilises one camera, while the second utilises a stereoscopic arrangement of two cameras.

2.2 Three–dimensional velocity measurement using one camera methodology

The schematic of the measuring principle of this method is shown in Figure 2. The position of the droplet in the laser sheet can be determined by the size of the fringe pattern in the resulting image, since its size is dependant on the distance of the droplet from the imaging lens and the size of the receiving aperture.

The apparent simplicity of this approach for position determination can still be hard in the case of a typical ILIDS system. It is common the area imaged by any typical system to not being parallel to the CCD array as imaging is required at a scattering angle θ, which is different than 90°. This results to images that have longer fringe patterns at one side of the image and shorter at the other. This can be solved by applying the Scheimpflug condition on the camera (Prasad & Jensen 1995), illustrated in Fig. 3. The Scheimpflug condition requires the planes of the laser sheet, the imaging lens and the imaging plane to intersect at one point in space. This allows for rotation of the field of

view, making the plane imaged to be parallel to the central plane of the laser sheet, instead of parallel to the imaging array. This means that the droplets that are physically on the same plane parallel to the laser sheet plane will have the same fringe pattern length in the resulting ILIDS image. This makes the depth position determination easier, since the only requirement is a way to correlate the length to the physical depth position. Certainly, an alternative approach to applying the Scheimpflug condition is performing fringe length interpolation along the horizontal direction of the ILIDS images, but this approach can be harder for depth determination since the fringe pattern length in this case is variable not only in the depth direction but also in the horizontal. In the context of the present contribution, only the Scheimpflug arrangement is considered.

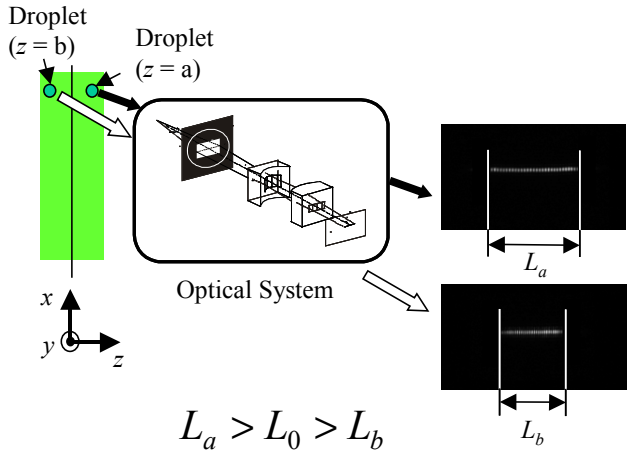

Fig. 2. The length of the fringe pattern is defined by the distance of the particle from the lens

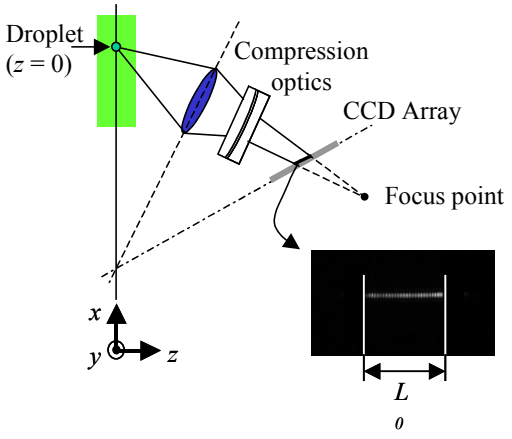

Fig. 3. The Scheimpflug condition imposes same–length fringe patterns for particles on the same z–plane position

To calibrate the one–camera Scheimpflug arrangement, an in–house built monodisperse droplet generator (Pergamalis, 2002) capable of producing a constant stream of equally spaced, one–size droplets can be traversed along the depth of the laser sheet. The length of the fringe patterns can then be measured in different depth locations along the laser sheet so that a mapping function for the fringe pattern length can be implemented. This function was decided to be a second–order polynomial dependent on the z–position of the droplet generator

$$L = c_0 + c_1 z + c_2 z^2 , \qquad (2)$$

and its c_i coefficients are calculated by least squares approximation.

2.3 Three–dimensional velocity measurement using two cameras methodology

The second method utilises a two–camera stereoscopic arrangement such as Steroscopic PIV (Prasad, 2000), illustrated in Figure 2. The 3D position is determined by matching the imaged particles on both views and measuring their depth position from translation of the image space to physical coordinates.

Given the nature of the position determination, the calibration information gathered for such a system is a crucial factor in the resulting measurement precision. As with the previous method, applying the Scheimpflug condition is helpful though not necessary. Images from a simple calibration plate can be used to map the physical space to the camera image space. To locate the nodes on such calibration images, the images can be cross–correlated with a circular template. The

cross–correlation peaks provide the dot centre image coordinates (*i,j*) and since the physical coordinates of the dots (*x, y,* z) are also known, one can map the physical coordinates to the image coordinates image (Willert & Gharib 1992). In the current contribution, this mapping function was chosen to be the following linear combination of the dot parameters

$$\begin{bmatrix} x \\ y \end{bmatrix} = \begin{bmatrix} a_0 & a_1 & a_2 & a_3 & a_4 & a_5 & a_6 & a_7 & a_8 & a_9 \\ b_0 & b_1 & b_2 & b_3 & b_4 & b_5 & b_6 & b_7 & b_8 & b_9 \end{bmatrix} \cdot \begin{bmatrix} 1 \\ i \\ j \\ z \\ i \cdot j \\ j \cdot z \\ i \cdot z \\ i^2 \\ j^2 \\ z^2 \end{bmatrix}. \tag{3}$$

By collecting as many dot centre coordinates as possible, a linear least squares approximation is possible for estimating the twenty coefficients a_i and b_i for each camera. Compared to the explicit model proposed by Willert & Gharib (1992), this mapping model has the advantage that the depth z–location is used implicitly.

By using the above model when the calibration coefficients are known, the position information can be extracted and validated by combining the information from both cameras. The flow chart of the image processing and the schematic of the coordinates extraction are shown in Fig. 4 and Fig. 5. The steps taken to determine the three–dimensional position are

(1) Calculation of the sizes and planar velocities for both camera frame pairs.
(2) Since for every particle *p* (*i,j*) are known, only *z* is required to determine *x* and *y*.
(3) To match the particle from camera 1, p_1, to the particle from camera 2, p_2, the diameter deviation must be lower that a predefined threshold
$$\left| \frac{d_1 - d_2}{d_1} \right| \leq d_{thresh}$$
(4) If step 3 holds, for the two particles to be identical, the quantity $X(p_1, p_2) = x(p_1) - x(p_2)$ has to be equal to zero. From $X(p_1, p_2) = 0$, z_{cand} is obtained.
(5) If for $z=z_{cand}$ $Y(p_1, p_2) = y(p_1) - y(p_2)$ is the candidate for which $Y(p_1, p_2)$ is closest to zero then $z=z_{cand}$ and p_1 is validated. If not, proceed to the next particle p_2 in step (3).
(6) If p_1 was not validated, proceed to the next particle from camera 1 at step (3).

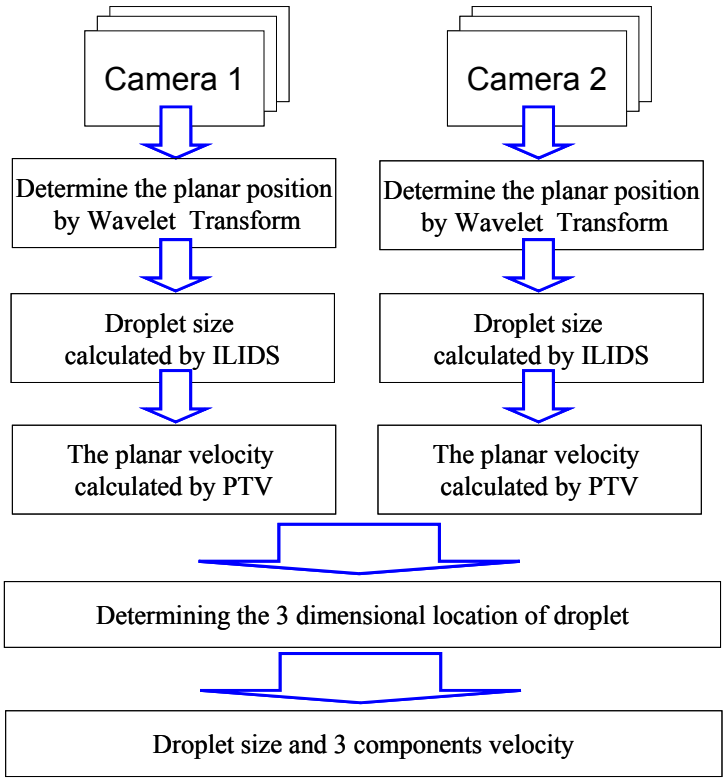

Fig. 4. Flow chart of the extraction of the size and three-component velocity process

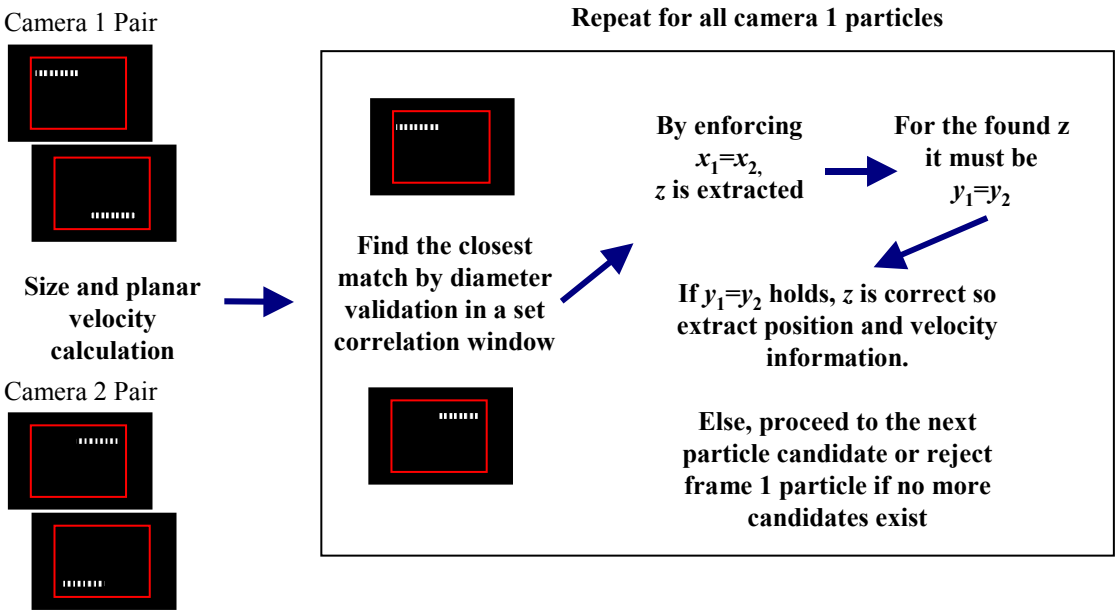

Fig. 5. Schematic of the coordinates extraction process

3. Measurement system

For the case of the two–camera arrangement, the measurement system schematic is shown in Fig. 6. It consisted of two CCD cameras (Kodak Megaplus ES4.0, 8bit, 2048×2048), positioned on Scheimpflug mounts, each bearing an objective lens (Nikon) with aperture mask and a pair of cylindrical lenses. To get highly visible interference, the scattering angle θ was set to 73°, where the intensity of the reflection and refraction is equal. The collecting angle α, which is equivalent to the angular inter–fringe spacing multiplied by the fringe count, was set to 6°. The specific cameras provide a field of view of approximately 20×20mm, which is twice the field of view of a typical ILIDS system. The light source was a dual pulsed Nd:YAG laser at a wavelength of 532nm, and its maximum output power is 120mJ/pulse. The thickness of the laser sheet was set to 3mm. The same system was employed for the one–camera arrangement.

For calibration purposes, a 20x20mm calibration plate was manufactured. Plate–through dots were drilled on its black surface so that the dot imaged by each camera is the same to the one imaged by the other. The dots where equally spaced with each other and in addition a depth step was introduced at both surfaces of the calibration plate so that two planes can be imaged simultaneously instead of one. The plate was traversed by a computer controlled mechanical linear 6μm/step–accurate stage in three different depth–positions of the laser sheet. By this procedure, the same three plane–pairs were imaged by both cameras along the laser sheet providing for a consistent physical–coordinates space mapping.

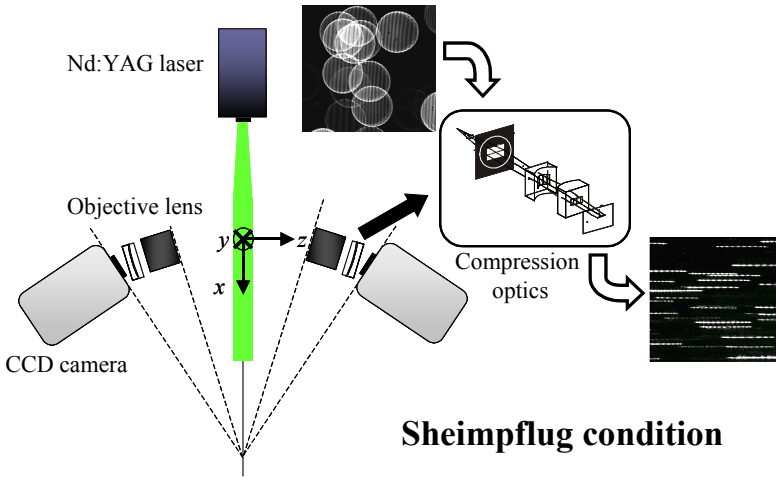

Fig. 6. Schematic of the measurement system

4. Results and Discussion

4.1 Verification of the effectiveness of Scheimpflug condition and fringe length function

To verify the effectiveness of the Scheimpflug condition and the fringe pattern length function along the depth position, the in–house monodisperse generator was traversed along the laser sheet. The monodisperse droplet generator atomising water at an injection pressure of 0.15Mpa, while the flow rate was $4.21\times10^{-8}m^3/s$ water. The resonance frequency of the piezoelectric elements of the monodisperse generator was set to 20 kHz. Under this condition, the diameter of the monodisperse is calculated to be approximately 159μm with an accuracy of 97% (Pergamalis, 2002).

The droplets from the monodisperse droplet generator were imaged at seven different positions along the z–direction and 5 positions along x direction. On each location, 20 images were acquired with a constant number of 20 droplets per one frame. The average fringe pattern length along the x–

position is shown in Fig. 7 and the averaged fringe pattern length along the *z*–position is shown in Fig. 8. Every point in Fig. 7 is the *x*–averaged fringe pattern length for the specific depth position. From Fig. 7, the pattern length uniformity due to the Scheimpflug condition is confirmed.

From Fig. 8, it is observed that the fringe length is proportional to the depth position, which ranges from 101 to 123 pixels within the 3mm laser sheet. Using this result, the function of the fringe pattern was estimated by equation (2)

$$L = 111.13 - 7.0715z - 111.13z^2 .$$

This results to a rather poor spatial resolution along the *z*–axis with approximately a displacement of 140μm for a fringe pattern change of only one pixel. Displacement automatically translates at a velocity resolution of over 7m/s for a typical time difference of 20μs between consecutive frames. It is made clear by this conclusion that the one–camera case has a large uncertainty in the position calculation, especially if the uncertainty in the pattern length determination by the image processing software is taken into account. Even so, the fringe pattern length along the depth direction is not useless information, as it can be used as an extra — although "rough" — validation criterion to the position determination when the stereoscopic arrangement is used.

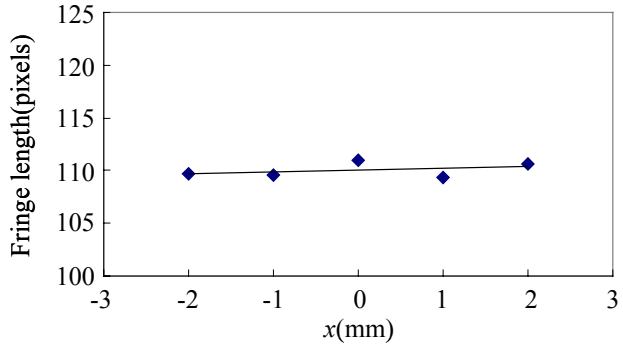

Fig. 7. The variation of the fringe pattern length along the *x*–direction

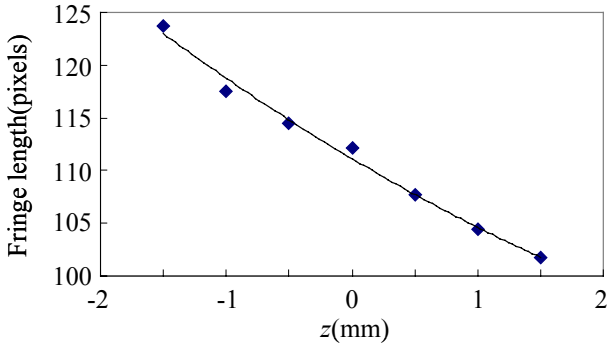

Fig. 8. The variation of the fringe pattern length along the *z*–direction

4.2 Verification the three–components velocity by the monodisperse droplet generator

The mono–disperse generator was also used to verify three components velocity. The condition of the monodisperse is the same to the aforementioned experiment. For this experiment the monodisperse generator was inclined at 75° in respect to horizontal axis on *z*-*y* plane. As already mentioned, for the one–camera arrangement it is difficult to estimate the velocity due to the poor depth–resolution. The average *z* position was calculated by the fringe pattern length function and the result is shown in Figure 9. The inclination was estimated to be 72° thus the error is approximately 3.9%.

In the stereoscopic arrangement, the instantaneous velocity vector map was calculated from 200 images. The two–dimensional vector on the *z*–*y* plane is presented in Fig. 10 while the three–dimensional vector is presented in Fig. 11. The depth velocity to axial velocity ratio was 4.05. The inclination in respect to the horizontal axis calculated by these ratios was estimated to be 76° for the *z*–*y* plane therefore the error is estimated at 1.5%. The droplet size was also measured. The probability density function of droplet size is exhibited in Figure 12. Most droplets are measured very closely to 165μm and the mean droplet diameter is 163.2μm so the error was estimated at 2.6%. Therefore the accuracy of this method is acceptable for the measurements of droplet size and three components velocity.

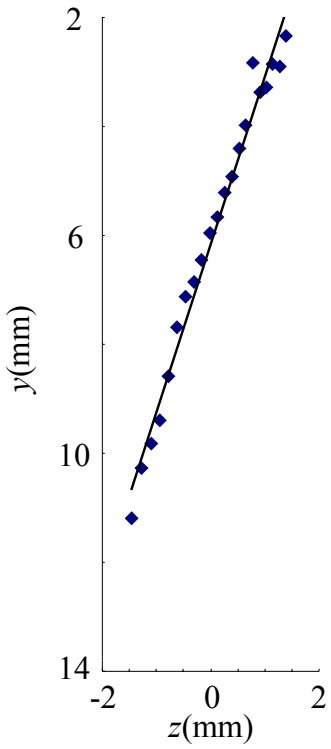

Fig. 9. The average droplet depth position as calculated from the function of their fringe pattern length

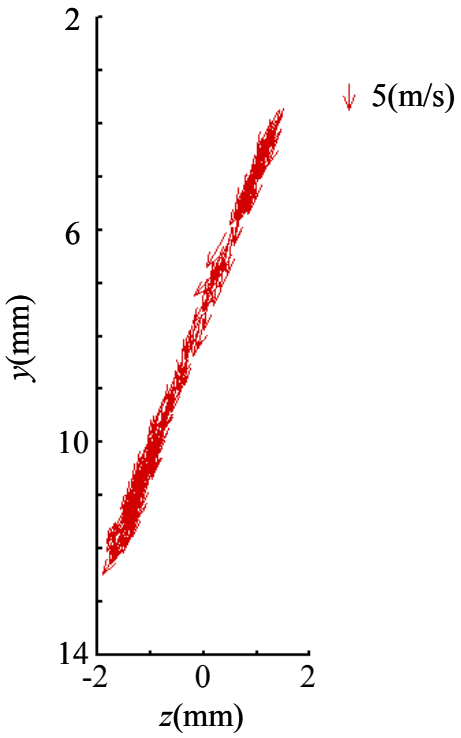

Fig. 10. The third component velocity of a 75° inclined monodisperse droplet generator of *z–y* plane

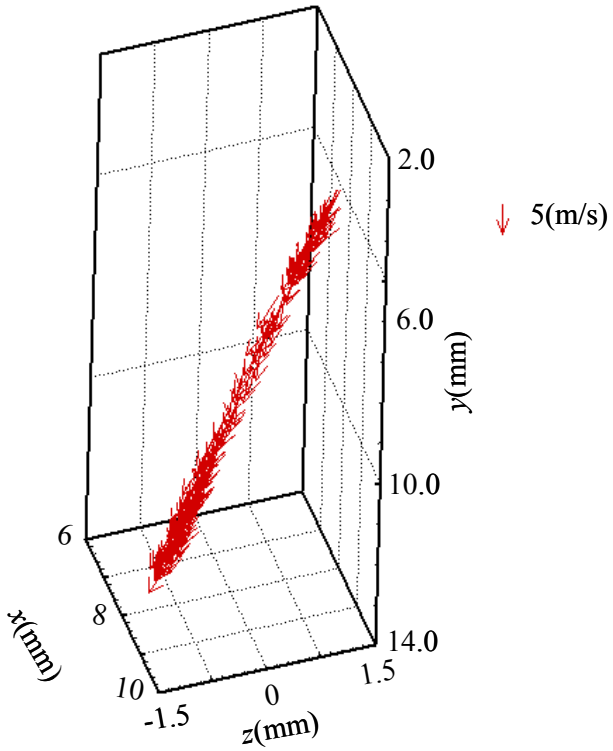

Fig. 11. The three–component velocity of a 75° inclined monodisperse droplet generator

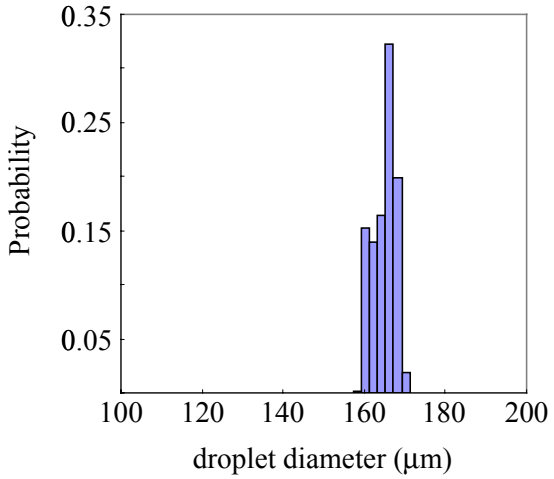

Fig. 12. Probability density distribution of the droplet diameter for the monodisperse flow

4.3 Experiments in dense spray

The stereoscopic method was applied on a typical spray flow created by a Delavan Type B solid cone nozzle with water injection pressure of 0.8MPa and a volumetric flow rate of $5.3\times10^{-7}m^3/s$ of water. The measurement location is shown in Fig. 13. The averaged three–component velocity vectors for the spray droplets whose diameter is larger than 40μm is presented in Fig. 14. The vector map shows that the droplets at each location move an almost same average velocity vector, which is approximately 1(m/s). The probability density distribution of the droplet diameter is shown in Fig. 15. The droplet size ranges from 25μm to 90μm. From these results, it is seen obvious that the method with stereoscopic method can be applied in typical sprays.

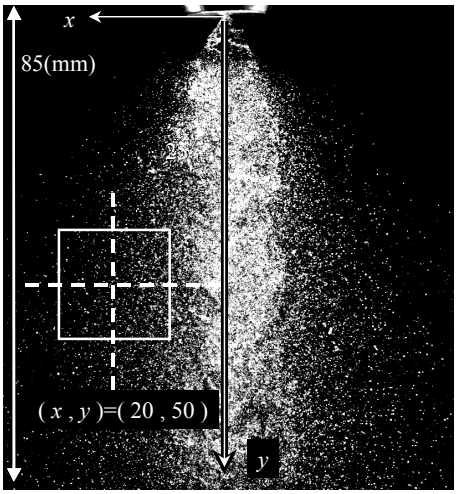

Fig. 13. Snapshot of the measured spray and measurement location

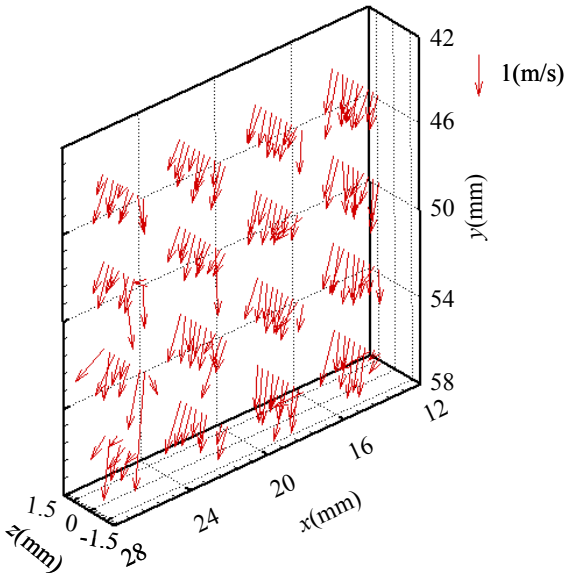

Fig. 14. The average three–component velocity for droplets in the spray whose diameter is more than 40 μm, at x = 20mm and y = 50mm

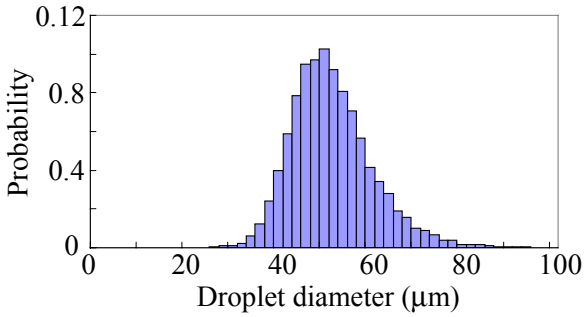

Fig. 15. Droplet diameter probability density distribution for the spray at location x = 20mm and y = 50mm

6. Conclusions

The interferometric laser imaging technique was extended to measure the three–component velocity and size of particles in two–phase flows. To achieve the third–component measurement of each droplet, two different methods were proposed to determine the three dimensional locations of each droplet; a single–camera arrangement and a two–camera stereoscopic arrangement. The first method calculates the particle depth position from its fringe pattern length, while the second by locating the particle in both camera views and extracting the depth–velocity from the combined information. Both approaches were tested on a piezoelectric monodisperse generator inclined to the laser sheet plane. The stereoscopic arrangement was also applied on a typical spray area. The main conclusions of the study are summarized below.

(1) To determine the three–dimensional location by using only one camera, the function of the fringe pattern length along the depth–position is estimated. The resolution along z–direction for the current system was approximately 140μm/pixel of only one pixel change to the fringe pattern length. This approach is not accurate enough to be applicable for measuring the three–component velocity of particles, but could be used in conjunction to the information from the calibration plate as an extra validation criterion for the stereoscopic arrangement.

(2) The stereoscopic arrangement that employs the Scheimpflug condition was used to measure a 15° inclined monodisperse droplet generator, to verify the droplet size and three–component velocity measurement accuracy. The error in the droplet sizing was estimated to be 2.6%. The inclination of the monodisperse generator was estimated 76° by the depth to axial velocity ratio, thus the error was 1.5%. These results indicate that the measurement system enables us to measure the droplet size and their three components velocity adequately.

(3) The method with stereoscopic arrangement was applied on a typical spray region. The distribution of the average three components velocity vectors was shown for particles with a diameter greater than 40 μm droplets. At each location the vectors are of the same size in the area of (x, y) =(20, 50), of approximately 1(m/s). For the droplet size measurements, the droplet size ranged from 25μm to 90μm at (x, y) =(20, 50). From these results, it is seen obvious that the method with stereoscopic method can be applied for a typical spray.

References

Damaschke N, Nobach H, Nonn TI, Semidetonv N, Tropea A (2001) Multi–dimensional particle sizing techniques. Exp Fluids 39:336–350

Glover AR, Skippon SM, Boyle RD (1995) Interferometric laser imaging for droplet sizing: A method for droplet–size measurement in sparse spray systems. Appl Opt 34:8409–8421

Hesselbacher KH, Anders K, Frohn A (1991) Experimental investigation of Gaussian beam effects on the accuracy of a droplet sizing method. Appl Opt 30:4930–4930

Kawaguchi T, Akasaka Y, Maeda M (2002) Size measurements of droplets and bubbles by advanced interferometric laser imaging technique. Meas Sci Technol 13:308–316

Maeda M, Kawaguchi T, Hishida K (2000) Novel interferometric measurement of size and velocity distribution of spherical particles in fluid flow. Meas Sci Technol 11:L13–L18

Maeda M, Akasaka Y, Kawaguchi T (2002) Improvements of the interferometric technique for simultaneous measurement of droplet size and velocity vector field and its application to a transient spray. Exp Fluids 33:125–134

Pergamalis H (2002) Droplet impingement onto quiescent and moving liquid surfaces. PhD Thesis, Imperial College London

Prasad AK, Jensen K (1995) Scheimpflug stereocamera for particle image velocimetry in liquid flows. Appl Opt 34:7092–7099

Roth N, Anders K, Frohn A (1991) Refractive–index measurement for the correction of particle sizing methods. Appl Opt 30:4960–4965

Van de Hulst HC, Wang RT (1991) Glare points. Appl Opt 30:4755–4763

Willert CE, Gharib M (1992) 3–dimensional particle imaging with a single camera. Exp Fluids 12:353–8

Zama Y, Kawahashi M, Hirahara H (2005) Simultaneous measurement method of size and 3D velocity components of droplets in a spray filed illuminated with a thin laser–light sheet. Meas Sci Technol 16:1977–1986